



LAWRENCE
LIVERMORE
NATIONAL
LABORATORY

The Location of the Maximum Temperature on the Cutting Edges of a Drill

M. J. Bono, J. Ni

February 9, 2005

International Journal of Machine Tools and Manufacture

Disclaimer

This document was prepared as an account of work sponsored by an agency of the United States Government. Neither the United States Government nor the University of California nor any of their employees, makes any warranty, express or implied, or assumes any legal liability or responsibility for the accuracy, completeness, or usefulness of any information, apparatus, product, or process disclosed, or represents that its use would not infringe privately owned rights. Reference herein to any specific commercial product, process, or service by trade name, trademark, manufacturer, or otherwise, does not necessarily constitute or imply its endorsement, recommendation, or favoring by the United States Government or the University of California. The views and opinions of authors expressed herein do not necessarily state or reflect those of the United States Government or the University of California, and shall not be used for advertising or product endorsement purposes.

The Location of the Maximum Temperature on the Cutting Edges of a Drill

Suggested Abbreviated Title:
Temperature Profile of a Drill

Matthew Bono*
Mechanical Engineer
Lawrence Livermore National Laboratory
7000 East Avenue
Livermore, CA 94550

Jun Ni
Professor
Department of Mechanical Engineering
University of Michigan
1023 H.H. Dow Building
2300 Hayward Street
Ann Arbor, MI 48109

*Corresponding author
Email: bono1@llnl.gov

Abstract

This study analyzes the temperature profile along the cutting edges of a drill and describes how the temperature on the chisel edge can exceed the temperature on the primary cutting edges. A finite element model predicts the temperature distribution in the drill, where the heat flux loads applied to the finite element model are determined from analytical equations. The model for the heat flux loads considers both the heat generated on the shear plane and the heat generated on the rake face of the tool to determine the amount of heat flowing into the tool on each segment of the cutting edges. Contrary to the conventional belief that the maximum temperature occurs near the outer corner of the drill, the model predicts that the maximum temperature occurs on the chisel edge, which is consistent with experimental measurements of the temperature profile.

Keywords

Drilling, metal cutting, temperature prediction, temperature measurement

Nomenclature

α	rake angle
α_t	thermal diffusivity of tool material
λ	inclination angle
η	chip angle
ϕ	shear angle
θ	angle between drill axis and the cutting edge
ρ_t	density of tool material
ρ_w	density of workpiece material
ω	angular velocity of the drill
c_t	heat capacity of tool material
c_w	heat capacity of workpiece material
F_c	component of the force on the ECT in the cutting direction
$F_{f,r}$	component of the force on the ECT in the direction of chip flow
F_z	component of the force on the ECT parallel to the drill axis
k_t	thermal conductivity of tool material
k_w	thermal conductivity of workpiece material
l_c	tool-chip contact length
q	total rate of heat generation for a simple cutting tool or an ECT
q''_{chip}	rate of heat flow into the chip per unit area over the tool-chip interface
$q_{friction}$	rate of heat generation by friction for a simple cutting tool or an ECT
$q''_{friction}$	rate of heat generation by friction per unit area on the tool-chip interface
q_{shear}	rate of heat generation in shear for a simple cutting tool or an ECT
q''_{tool}	rate of heat flow into the tool per unit area over the tool-chip interface
R_2	fraction of heat generated on rake face that is conducted into the chip
$(1-R_2)$	fraction of heat generated on rake face that is conducted into the tool
T	torque contributed by an ECT = $(F_c)(radius)$
t	time
t_2	chip thickness
T_o	ambient temperature
T_{chip}	average temperature of the chip over the tool-chip contact area
T_{tool}	average temperature of the tool over the tool-chip contact area
$T_i(x,t)$	temperature in a semi-infinite body subject to uniform surface heat flux
ΔT_s	average temperature rise of the shear plane
V_{cut}	cutting velocity = $(\omega)(radius)$
V_{chip}	chip velocity
V_f	feed velocity of the drill
w	width of cut

1. Introduction

The significance of developing predictive and experimental methods for analyzing the temperatures of cutting tools has long been recognized. The temperatures associated with the drilling process are particularly important, because drilling is one of the predominant industrial machining processes, and heat effects in drilling are generally more severe than in other metal cutting operations. Drills often experience excessive temperatures, because the drill is embedded in the workpiece, and heat generation is localized in a small area. The resulting temperatures can lead to accelerated tool wear and reduced tool life, and they can have profound effects on the overall quality of the machined workpiece. Drill designers often select the geometrical features of a drill based on the expected temperature profile in the drill point, so accurate prediction of the temperature distribution is imperative.

A great deal of research has been performed on this topic, and many previous researchers have developed models for predicting drill temperature. Hervey and Cook [1] developed a model for the average temperature along the cutting edges of a drill. DeVries et al. [2] developed a more sophisticated analytical model for the temperature distribution along the cutting edges. Agapiou and DeVries [3,4] extended this work and developed an analytical model for the transient temperature distribution in a twist drill that addressed many of the limitations inherent in previous models. Their model was based on the calculation of the temperature of the chip at the tool-chip interface. Their model was then improved by Agapiou and Stephenson [5], who extended the analytical model to calculate transient and steady-state temperature distributions for drills with arbitrary point geometries. These analytical models have generally analyzed the flow of heat and the temperature distribution in the tool by treating the drill as a semi-infinite body.

Several researchers have developed models that consider the complex geometry of the drill and combine analytical and numerical methods to calculate the temperature distribution throughout the drill [6-11]. These methods use finite difference or finite element models to calculate drill temperature, where the heat flux loads applied to the model are calculated from analytical equations for the flow of heat into a cutting tool. This combined approach has proven to be a powerful method that is relatively simple to implement.

Each of the previously developed combined analytical/numerical models for drill temperature requires an analysis of the amount of heat that flows into the tool over the tool-chip contact area. In each of these previous models, the calculation of the heat that flows into the tool consists of two primary steps. In the first step, the amount of heat generated by friction on the rake face of the tool is calculated, where the heat generated on the rake face is a function of the product of the chip velocity and the component of the resultant force on the tool in the direction of chip flow. In the second step, the partition of this heat between the chip and the tool is calculated. This heat partition is usually calculated using the model developed by Loewen and Shaw [12]. The heat flux load applied to the tool is determined by multiplying the heat generated on the rake face by the fraction of that heat that flows into the tool and dividing by the area of contact.

The temperature distributions along the cutting edges of the drill predicted by these previous studies [2,3,6-11] share similar characteristics. Each method predicts that the maximum cutting edge temperature occurs on or near the ends of the primary cutting edges of the drill. However, these predicted temperature distributions contradict some experimentally measured temperature profiles.

The experimental measurements of several researchers indicate that either the temperature is nearly uniform along the cutting edges, or the maximum drill temperature occurs on or near the chisel edge of the drill. DeVries et al. [2] measured the temperature profile near the cutting edges using thermocouples embedded in the drill flank. They noted that their measured temperatures were much larger than the predicted temperatures near the chisel edge, and in some cases, they measured nearly flat temperature profiles in which the temperatures increased near the chisel edge. Watanabe et al. [7] measured the drill temperature profile using an embedded wire tool-work thermocouple and found a nearly flat temperature profile. Mills and Mottishaw [13] measured the drill temperature profile by examining microstructural changes in the drill material, and they found that the highest temperatures occurred near the axis of the drill. Experimental studies by the authors of the current study using drill-foil thermocouples [14,15] have also revealed that the maximum drill temperature can occur on the chisel edge.

This discrepancy, in which previous models have predicted that the maximum temperature occurs near the ends of the primary cutting edges, and experimental measurements reveal that the maximum temperature occurs near the chisel edge, indicates a limitation of the previous predictive methods. The objective of the current study is to analyze the temperature profile along the cutting edges of a drill and provide a theoretical explanation for the fact that the maximum temperature can occur near the chisel edge.

The current study uses a finite element analysis (FEA) to calculate the temperature distribution in the drill. The heat flux loads applied to the finite element model are calculated from analytical equations, which is the same general type of approach used in several previous numerical studies [7-11]. However, the current study develops a different method for calculating the heat flux loads. Unlike the previous numerical studies, which calculated the heat flux loads on the drill by assuming they are a fraction of the heat flux generated by frictional shearing on the rake face of the tool, the current model considers both the frictional heat and the heat generated on the shear plane.

Contrary to the conventional belief that the maximum temperature of a drill occurs near the outer corner, the current model and experimental measurements indicate that the maximum temperature can occur on the chisel edge. This result could have important implications on the way in which certain drills are designed. Traditionally, performance problems related to excessive drill temperatures, such as severe build-up in the dry drilling of aluminum, have been addressed by altering the design of the outer corner of the drill. However, the current research indicates that the design of the chisel edge portion of the drill could have the greatest effect on the maximum drill temperature.

2. Model for Drill Temperature

2.1 Finite Element Model of the Drill

This study analyzes the case in which a high-speed steel drill of diameter 9.92 mm machines a hole in a workpiece of aluminum 319. The temperature distribution in the drill is calculated using a finite element analysis created with the commercial finite element code ABAQUS Standard. A three-dimensional finite element model of the drill consisting of eight-node diffusive heat transfer elements of type DC3D8 is illustrated in Fig. 1. The model is

identical to the drills used in the experiments. The heat that enters the drill is modeled by applying heat flux to the elements on the chisel edge and primary cutting edges of the drill. All other surfaces of the model are adiabatic.

Because the temperature of the drill increases near the point but remains relatively constant near the shank, it is not necessary to model the entire length of the drill. Thus, only one-third of the drill is modeled in the finite element analysis. The nodes are spaced so that the elements are small near the drill point, where the temperature gradients are large [8]. The temperature gradients decrease with distance from the cutting edges, so larger elements are used for the remainder of the drill. To ensure that the heat flux loads are applied over an appropriately sized area, the sizes of the elements on the rake face of the primary cutting edges and the chisel edge are selected based on the calculated tool-chip contact length for each elementary cutting tool (ECT).

During initial entry of the drill into the workpiece, the drill is not fully engaged, and only part of the drill performs cutting. Therefore, during the initial entry of the drill, the model applies heat flux only to those elements that are in contact with the workpiece. As the drill progresses deeper into the workpiece, heat flux is appropriately applied to elements as they engage in cutting.

2.2 Analysis of the Heat Flowing Into the Drill

2.2.1 Heat Generated on the Rake Face of the Tool

To calculate the heat flux loads on each of the elements of the finite element model, the cutting edges of the drill are considered as a sequence of individual, elementary cutting tools. As shown in Fig. 2, each elementary cutting tool performs a simple metal cutting operation. Thus, metal cutting theories can be used to evaluate the forces and heat transfer on each segment of the cutting edge.

The drills used in this study were ground to a prescribed geometry, so all of the geometrical features, including the rake angle and inclination angle, are known for each ECT. In addition, the thrust force and cutting force for each ECT are calculated using the mechanistic model created by Chandrasekharan and coworkers [16,17] and modified by Chen [18], which considers the variation in cutting geometry along the cutting edges of the drill. Thus, for each ECT, the thrust force, F_z , and the cutting force, F_c , are known quantities.

As in any metal cutting problem, the majority of the machining energy consumed by each ECT is contributed by plastic deformation on the shear plane and friction on the rake face of the tool [19]. Energy is also consumed by other factors, including ploughing, flank wear, and the creation of new material surface. However, the energy consumed by these other effects is relatively small. Thus, the total amount of heat generated by each ECT is a function of the rate of heat generated in shear and the rate of heat generated by friction, and it can be calculated from the forces acting on the ECT.

$$q = q_{shear} + q_{friction} = T \cdot \omega + F_z \cdot V_f \quad (1)$$

The rate of heat generated by friction on the rake face of the ECT is given by Eq. (2).

$$q_{friction} = F_{f,r} V_{chip} \quad (2)$$

$F_{f,r}$ is the force acting on the ECT in the direction of chip flow, which can be related to the known force components F_z and F_c using a geometrical analysis of oblique cutting [20]. First,

F_t , which is the force on the ECT perpendicular to the plane defined by the cutting edge and the tool velocity, must be calculated as a function of F_z and F_c .

$$F_t = \frac{F_z + F_c \cdot a}{b} \quad (3)$$

$$a = \frac{\sin \lambda - \cos \lambda \sin \alpha \tan \eta}{\sin \lambda \sin \alpha \tan \eta + \cos \lambda} \cdot \frac{\cos \theta}{\cos \lambda} \quad (4)$$

$$b = \frac{\cos \alpha \tan \eta}{\sin \lambda \sin \alpha \tan \eta + \cos \lambda} \cdot \frac{\cos \theta}{\cos \lambda} + \frac{\sqrt{\cos^2 \lambda - \cos^2 \theta}}{\cos \lambda} \quad (5)$$

$F_{f,r}$ can then be geometrically related to F_t and F_c , as described by Eq. (6).

$$F_{f,r} = \frac{(\cos \alpha \cos \lambda) \cdot F_t + (\sin \alpha) \cdot F_c}{\cos^2 \alpha \cos \lambda \cos \eta + \sin \alpha \cdot (\sin \lambda \sin \eta + \sin \alpha \cos \lambda \cos \eta)} \quad (6)$$

V_{chip} is the chip velocity, which can be geometrically related to the cutting velocity [19].

$$V_{chip} = V_{cut} \cdot \frac{\cos \lambda \sin \phi}{\cos \eta \cos(\phi - \alpha)} \quad (7)$$

The chip angle is found from Stabler's flow rule, which states that the chip angle is approximately equal to the inclination angle. The shear angle, ϕ , and the contact length, l_c , must also be calculated for each ECT. Relations for ϕ and l_c corresponding to a high-speed steel tool and a workpiece of aluminum 319 are determined from experimental turning test data [21].

$$\phi = 0.3697 \cdot \alpha + 0.4667 [rad] \quad (8)$$

$$l_c = 4.27 \cdot t_2 \quad (9)$$

2.2.2 Flow of Heat Into the Chip and the Tool

The plastic deformation on the shear plane is also an important source of heat generation in metal cutting. A portion of this heat enters the chip and raises its temperature, which subsequently affects the partition of heat as the chip slides along the rake face of the tool. A schematic diagram of the heat transfer that occurs over the tool-chip contact area appears in Fig. 3.

This heat transfer problem can be analyzed by making several simplifying assumptions [3]. The heat generated on the shear plane is assumed to raise the average shear plane temperature by an amount ΔT_s above the ambient temperature. A heat flux, $q''_{friction}$, is generated by the frictional interaction between the chip and the tool. Note that $q''_{friction}$ is simply $q_{friction}$ divided by the tool-chip contact area. A net heat flux q''_{chip} enters the chip and changes the average interface temperature on the chip to T_{chip} , and a net heat flux q''_{tool} enters the tool and changes the average interface temperature on the tool to T_{tool} . This study idealizes these heat fluxes and assumes they are uniform over the tool-chip contact area for each ECT. An energy balance over the interface region requires that the total amount of heat flux generated be equal to the sum of q''_{chip} and q''_{tool} , as described by Eq. (10).

$$q''_{friction} = q''_{chip} + q''_{tool} \quad (10)$$

The transient temperature of the rake face of the tool can be estimated by treating the tool as a semi-infinite body [3]. The temperature rise at a depth, x , below the surface of a semi-infinite body subject to a uniform, constant surface heat flux, q''_o , is given by Eq. (11) [22].

$$T_t(x, t) - T_o = \frac{2q''_o (\alpha_t t / \pi)^{1/2}}{k_t} \exp\left(\frac{-x^2}{4\alpha_t t}\right) - \frac{q''_o x}{k_t} \operatorname{erfc}\left(\frac{x}{2\sqrt{\alpha_t t}}\right) \quad (11)$$

Thus, the average temperature of the tool over the tool-chip contact area at time t can be estimated using Eq. (12).

$$T_{tool} = T_o + 2q''_{tool} \sqrt{\frac{t}{\pi k_t \rho_t c_t}} \quad (12)$$

The average temperature of the chip over the tool-chip contact area can be estimated using Jaeger's solution for the average temperature beneath a frictional slider dissipating uniform heat flux as it slides with constant velocity over the surface of a semi-infinite body [12]. Thus, the average temperature of the chip over the tool-chip contact area can be estimated from Eq. (13).

$$T_{chip} = T_o + \Delta T_s + 0.754 \cdot q''_{chip} \sqrt{\frac{l_c}{V_{chip} k_w \rho_w c_w}} \quad (13)$$

Note that the average interface temperature of the tool must be equal to the average interface temperature of the chip [12]. Setting Eq. (12) equal to Eq. (13) and inserting Eq. (10) leads to the following expression for the heat flux into the tool.

$$q''_{tool} = \frac{\Delta T_s + q''_{friction} L_{chip}}{L_{tool} + L_{chip}} \quad (14)$$

The parameters, L_{chip} and L_{tool} , are defined in Eq. (15) and Eq. (16).

$$L_{chip} \equiv 0.754 \sqrt{\frac{l_c}{V_{chip} k_w \rho_w c_w}} \quad (15)$$

$$L_{tool} \equiv 2 \sqrt{\frac{t}{\pi k_t \rho_t c_t}} \quad (16)$$

Note that in the current analysis, the heat flux into the tool is a function of both the shear plane temperature and the heat generated by the frictional interaction between the chip and the tool. Therefore, the heat flux loads applied to the FEA of the drill in the current study differ from those applied to the drill in previous numerical studies of drill temperature, which assumed the heat flux into the drill is simply a fraction of the heat flux generated by friction on the rake face of the tool.

The heat flux into the chip is given by Eq. (17). Note that the current analysis allows for the possibility that heat may flow either into or out of the chip over the tool-chip contact area. If the quantity $q''_{friction} L_{tool}$ is larger than ΔT_s , then heat will flow into the chip over the tool-chip interface. However, if ΔT_s is larger than the quantity $q''_{friction} L_{tool}$, then the chip will lose heat over the tool-chip contact area.

$$q''_{chip} = \frac{q''_{friction} L_{tool} - \Delta T_s}{L_{tool} + L_{chip}} \quad (17)$$

The current study estimates ΔT_s using the analytical equations presented by Agapiou and DeVries [3], which calculate the transient temperature in the shear zone using the classical frictional slider model that treats the workpiece as a semi-infinite solid.

3. Results

The model described above is used to calculate the temperature distribution in a drill during the drilling process. The heat flux loads applied to the drill are calculated using Eq. (14). This study analyzes the case in which a high-speed steel drill of diameter 9.92 mm produces a hole in a workpiece of aluminum 319 to a depth of 25 mm using a speed of 998 rpm and feed of 124 microns per revolution. The predicted temperature rises at each of the nodes along the chisel edge and primary cutting edges of the drill are plotted as the solid dots in Fig. 4. In addition, to illustrate how the temperature distribution predicted by the current model differs from that predicted by previous methods, another simulation is performed using heat flux loads that are calculated using Eq. (18). The previous numerical studies of drill temperature calculated the heat flux loads on the drill using an expression similar to Eq. (18).

$$q''_{tool} = q''_{friction} (1 - R_2) = \frac{(1 - R_2) F_{f,r} V_{chip}}{l_c w}, \quad 0 \leq R_2 \leq 1 \quad (18)$$

R_2 is defined as the fraction of the friction heat that flows into the chip. $(1 - R_2)$ is the fraction of the friction heat that flows into the tool and is usually calculated using the model developed by Loewen and Shaw [12]. Because R_2 represents a fraction, it is restricted to values between 0 and 1.

It is interesting to note the similarity between the current analysis of the heat flux on the tool and that of Agapiou and DeVries [3]. If the expression for R_2 developed in their analysis were inserted into Eq. (18), and if the restriction were removed so that R_2 could take on any value, then the resulting equation would be nearly identical to Eq. (14). In other words, the only significant difference between the analysis of the heat flux developed in the current study and that developed by Agapiou and DeVries [3] is that the current study avoids the intermediate term, R_2 .

The temperature rises at each of the nodes along the cutting edges predicted using Eq. (18) are plotted as the open triangles in Fig. 4. The solid line in the figure represents the temperature distribution along the cutting edges measured using a drill-foil thermocouple [14], which measures the electromotive force generated between the cutting tool and an insulated foil embedded in the workpiece. By calibrating the measured voltage with the temperature at the interface of the dissimilar metals, the temperature profile along the entire cutting edge is determined as the drill point passes through the foil. All of the data in Fig. 4 correspond to a drilling depth of 25 mm.

The current analysis is a simplified treatment of the heat generated in the metal cutting process and is based on a large number of assumptions. For example, the analytical equations treat the bodies as semi-infinite solids, the temperature dependence of the thermal properties of the tool and workpiece are neglected, and rubbing on the drill flank is ignored, to name but a few. Therefore, as is typical of models for drill temperature, the current model is unable to accurately predict the magnitude of the temperature rise for a general drilling scenario. However, recall that the current study is primarily concerned with the shape of the temperature profile and the location of the maximum temperature. Therefore, the predicted and measured temperature profiles are presented in a different manner in Fig. 5. In this figure, each of the temperature profiles has been normalized by dividing by the corresponding average temperature on the primary cutting edges. The predicted normalized temperature distributions throughout the drill point are illustrated in Fig. 6.

As shown in Fig. 5 and Fig. 6, the shape of the temperature profile along the cutting edges predicted by the current model is similar to the measured temperature profile. In both the measured profile and the profile predicted using the current model, the maximum temperature occurs on the chisel edge, and the temperature decreases with radius and reaches its minimum value near the ends of the primary cutting edges. In contrast, the temperature profile predicted by the method used by previous researchers presented in Eq. (18) has a very different shape. In this profile, the temperature on the chisel edge is significantly lower than the temperature on the primary cutting edges.

In summary, the current model predicts a temperature profile in the drill point that is consistent with experimental data, in which the maximum temperature occurs on the chisel edge [13,14]. In contrast, simulations that are based on the method presented in previous studies, in which the heat flowing into the tool is simply assumed to be a fraction of the heat generated by friction on the rake face of the tool, predict that the temperature on the chisel edge is significantly lower than on the primary cutting edges. In the chisel edge area, the heat generated by the frictional interaction between the chip and the tool is relatively small, because the chip velocity and the cutting torque are small. However, the shear plane temperature is often larger on the chisel edge than on the primary cutting edges, and a portion of the shear plane heat can be transferred into the tool via the chip. For example, for the drilling scenario discussed above, the predicted shear plane temperature resulting from the negative rake angle on the chisel edge is approximately 370 °C, but the predicted shear plane temperature on the primary cutting edge ranges from only 150 °C to 200 °C. The larger shear plane temperature results in greater preheating of the chip at the shear plane, with the result that more heat flows into the drill on the chisel edge. Therefore, accurate prediction of the shape of the temperature profile in the drill requires consideration of both the heat generated on the shear plane and the heat generated by the frictional interaction between the chip and the tool.

4. Conclusions

This study analyzes the temperature profile along the cutting edges of a drill and provides a theoretical explanation for the fact that the maximum temperature can occur near the chisel edge. Analytical equations are developed to calculate the heat flux loads applied to a finite element model of the drill. For each of the elementary cutting tools on the drill, the heat generated on the shear plane directly affects the temperature of the chip at the shear plane and the flow of heat at the rake face of the tool. The drilling scenario analyzed in this study exemplifies that the manner in which this heat source is treated in the analysis affects the shape of the predicted temperature profile along the cutting edges. In this study, the results predicted by the model are consistent with experimental observations, in which the temperature near the chisel edge is larger than on the primary cutting edges.

Acknowledgement

This work was performed under the auspices of the U.S. Department of Energy by University of California, Lawrence Livermore National Laboratory under Contract W-7405-Eng-48. This work was also supported in part by the Engineering Research Program of the Office of Basic Energy Sciences at the Department of Energy.

References

- [1] R. Hervey, N. Cook, Thermal parameters in drill tool life, ASME paper 65-Prod-15, 1965.
- [2] M.F. DeVries, U.K. Saxena, S.M. Wu, Temperature distributions in drilling, *Journal of Engineering for Industry* 90 (1968) 231-238.
- [3] J.S. Agapiou, M.F. DeVries, On the determination of thermal phenomena during drilling - Part I - Analytical models of twist drill temperature distributions, *International Journal of Machine Tools and Manufacture* 30 (1990) 203-215.
- [4] J.S. Agapiou, M.F. DeVries, On the determination of thermal phenomena during drilling - Part II - Comparison of experimental and analytical twist drill temperature distributions, *International Journal of Machine Tools and Manufacture* 30 (1990) 217-226.
- [5] J.S. Agapiou, D.A. Stephenson, Analytical and experimental studies of drill temperatures, *Journal of Engineering for Industry* 116 (1994) 54-60.
- [6] U.K. Saxena, M.F. DeVries, S.M. Wu, Drill temperature distributions by numerical solutions, *Journal of Engineering for Industry* (1971) 1057-1066.
- [7] K. Watanabe, K. Yokoyama, R. Ichimiya, Thermal analysis of the drilling process, *Bulletin of the Japan Society for Precision Engineering* 11 (1977) 71-77.
- [8] K.H. Fuh, W.C. Chen, P.W. Liang, Temperature rise in twist drills with a finite element approach, *International Communications in Heat and Mass Transfer* 21 (1994) 345-358.
- [9] W. Chen, Effect of the cross-sectional shape design of a drill body on drill temperature distributions, *International Communications in Heat and Mass Transfer* 23 (1996) 355-366.
- [10] Q. Shen, T. Lee, W. Lau, A finite-element analysis of temperature distributions in spade drilling, *Journal of Materials Processing Technology* 66 (1997) 112-122.
- [11] M. Bono, J. Ni, The effects of thermal distortions on the diameter and cylindricity of dry drilled holes, *International Journal of Machine Tools and Manufacture* 41 (2001) 2261-2270.
- [12] E.G. Loewen, M.C. Shaw, On the analysis of cutting-tool temperatures, *Transactions of the A.S.M.E.* 76 (1954) 217-231.
- [13] B. Mills, T.D. Mottishaw, The application of scanning electron microscopy to the study of temperatures and temperature distributions in M2 high speed steel twist drills, *Annals of the C.I.R.P.* 30 (1981) 15-20.
- [14] M. Bono, J. Ni, A method for measuring the temperature distribution along the cutting edges of a drill, To appear in the *Journal of Manufacturing Science and Engineering*.
- [15] M. Bono, Experimental and Analytical Issues in Drilling, Diss. University of Michigan 2002.
- [16] V. Chandrasekharan, A Model To Predict The Three-Dimensional Cutting Force System For Drilling With Arbitrary Point Geometry, Diss. University of Illinois at Urbana-Champaign 1996.
- [17] V. Chandrasekharan, S.G. Kapoor, R.E. DeVor, A mechanistic model to predict the cutting force system for arbitrary drill point geometry, *Journal of Manufacturing Science and Engineering* 120 (1998) 563-570.
- [18] Y. Chen, Modeling For New Drilling Process Development, Diss. University of Michigan 1999.
- [19] M.C. Shaw, *Metal Cutting Principles*, Oxford University Press, 1984.

- [20] M. Bono, J. Ni, A model for predicting the flow of heat into the workpiece in dry drilling, To appear in the Journal of Manufacturing Science and Engineering.
- [21] L. Zhang, Diss. University of Michigan 2002.
- [22] F. Incropera, D. DeWitt, Fundamentals of Heat and Mass Transfer, John Wiley and Sons, Inc., 1990.

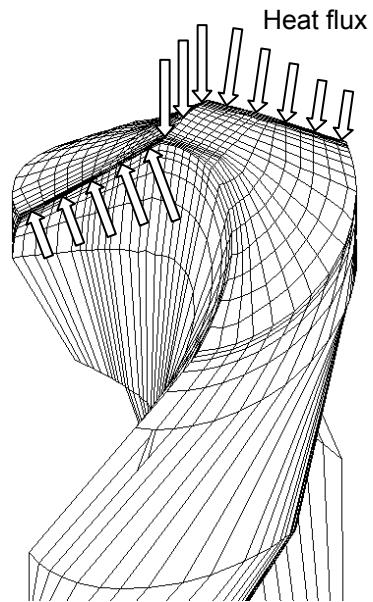


Fig. 1. Finite element model of the drill and the heat flux loads

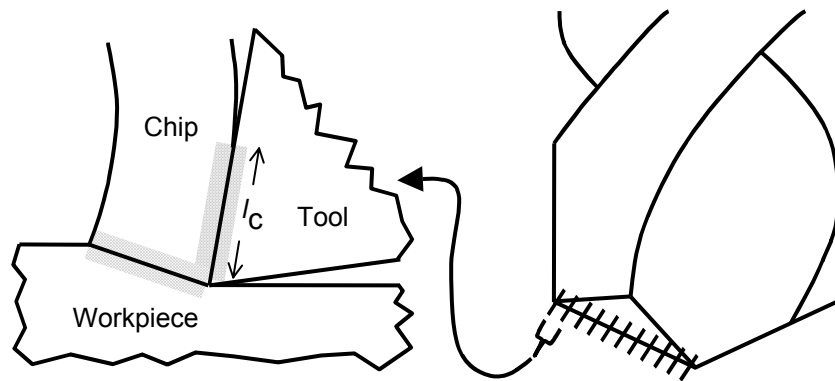


Fig. 2. Elementary cutting tools along the cutting edges of the drill

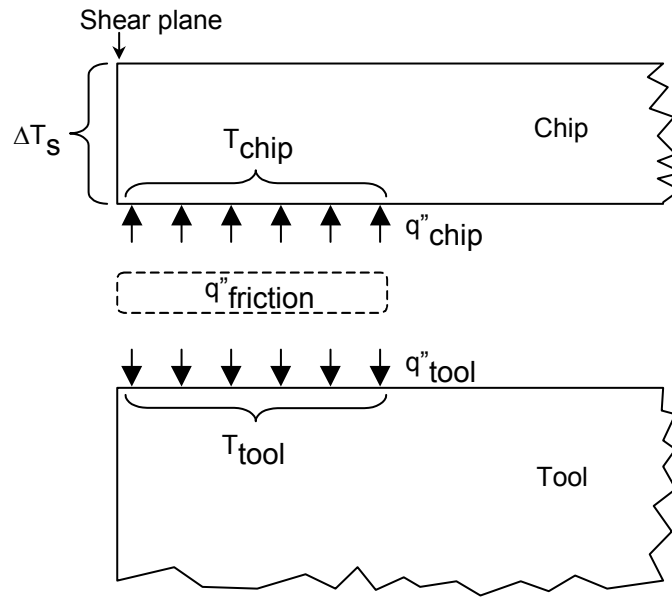


Fig. 3. Schematic diagram of the heat transfer over the tool-chip contact area

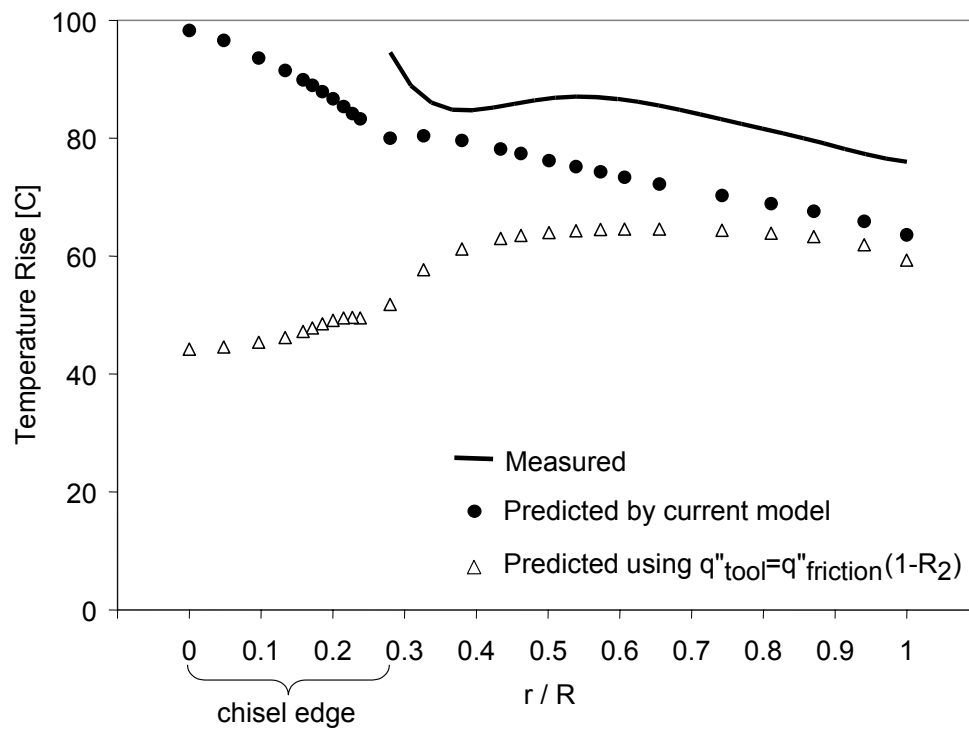


Fig. 4. Measured and predicted temperature profiles along the cutting edges of the drill at a drilling depth of 25 mm

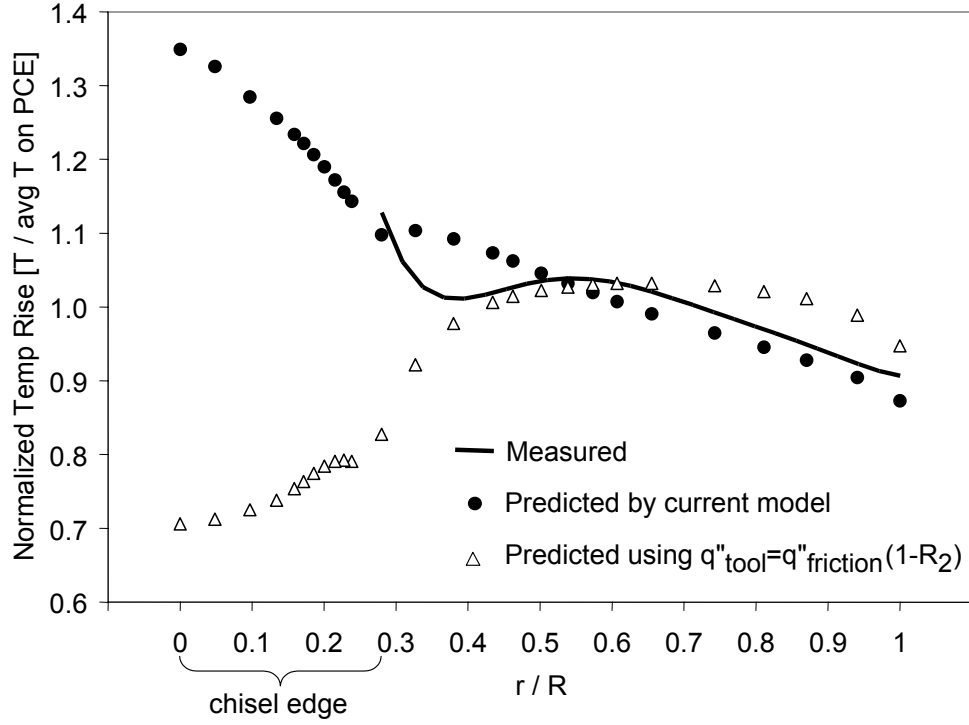


Fig. 5. Measured and predicted normalized temperature profiles along the cutting edges of the drill at a drilling depth of 25 mm

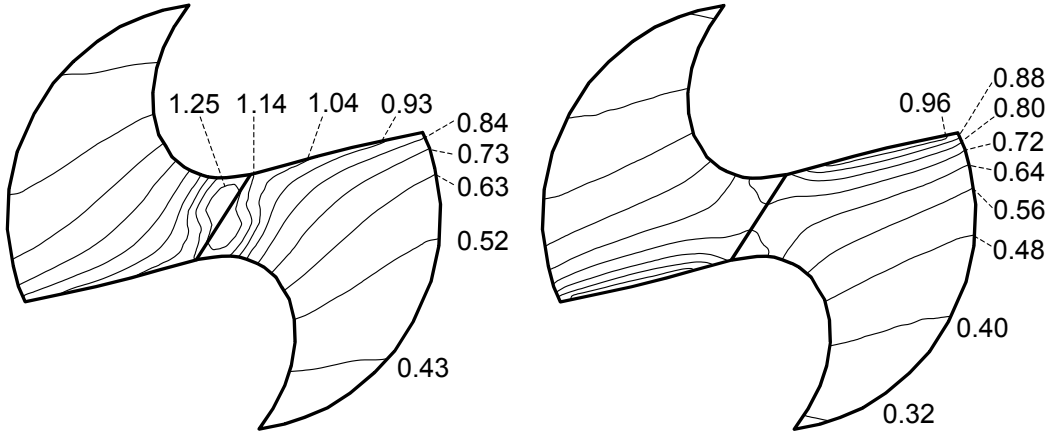


Fig. 6. Predicted normalized temperature distributions in the drill point at a drilling depth of 25 mm using Eq. (14) [left] and Eq. (18) [right]